Teske, A., Lizarralde, D., Höfig, T.W., and the Expedition 385 Scientists
Proceedings of the International Ocean Discovery Program Volume 385
publications.iodp.org

Data report: concentration and carbon isotopic composition in pore fluids from IODP Expedition 385[1]

Marta E. Torres[2] and Ji-Hoon Kim[3]

[1] Torres, M.E., and Kim, J.-H., 2022. Data report: concentration and carbon isotopic composition in pore fluids from IODP Expedition 385. In Teske, A., Lizarralde, D., Höfig, T.W., and the Expedition 385 Scientists, Guaymas Basin Tectonics and Biosphere. Proceedings of the International Ocean Discovery Program, 385: College Station, TX (International Ocean Discovery Program). http://doi.org/10.14379/iodp.proc.385.201.2022
[2] College of Earth, Ocean and Atmospheric Science, Oregon State University, USA. **marta.torres@oregonstate.edu**
[3] Marine Geology and Energy Division, Korea Institute of Geoscience and Mineral Resources, Republic of Korea.

Contents

Keywords
International Ocean Discovery Program, IODP, *JOIDES Resolution*, Expedition 385, Guaymas Basin Tectonics and Biosphere, Site U1545, Site U1546, Site U1547, Site U1548, Site U1549, Site U1550, Site U1552, dissolved carbon concentration and isotopes

References (RIS)

MS 385-201
Received 12 April 2022
Accepted 14 June 2022
Published 3 October 2022

Abstract

During International Ocean Discovery Program (IODP) Expedition 385, sediments from Guaymas Basin were sampled with the goal of understanding the role of sill emplacement and fluid flow, as well as its associated temperature and fluid circulation regimes, on subsurface carbon mobilization and preservation of organic-rich sediments. We report on the concentration and isotopic composition of dissolved inorganic carbon (DIC) in pore fluids from Sites U1545 and U1546, which were drilled in the northern basin; Sites U1547 and U1548, which sampled an active hydrothermal vent site; Sites U1549 and U1552, which targeted cold seeps; and Site U1550, which was drilled in the axial trough. There is large variability in the DIC concentrations. The highest values were recorded at Sites U1549, U1550 (up to ~75 mM), and U1552 (~169 mM). The isotopic composition of the DIC ($\delta^{13}C_{DIC}$) ranges −23.50‰ to 22.64‰ referenced to Vienna Peedee belemnite. At all locations outside Ringvent Site U1547, depletions in $\delta^{13}C_{DIC}$ values typically coincide with the sulfate–methane transition zone (SMTZ). Enrichment in $\delta^{13}C_{DIC}$ above seawater values, indicative of ongoing microbial methanogenesis, was recorded below the SMTZ at all locations except Ringvent.

1. Introduction

During International Ocean Discovery Program (IODP) Expedition 385, eight sites were drilled in Guaymas Basin with the broad goal of unraveling the physical, chemical, and biological processes that regulate the cycling of sedimentary carbon in a region where extensive chemical, temperature, and lithologic gradients impact both biotic and abiotic processes that release and/or sequester carbon in the sediment (**Teske et al.**, 2021a). Emplaced volcanic sills that originate at the spreading center significantly alter the host sediment and control hydrothermal circulation patterns in Guaymas Basin (Einsele et al., 1980). Hydrothermal alteration of buried carbon mobilizes and delivers hydrocarbons and methane to the biosphere, a process that could have relevance on climate history (Lizarralde et al., 2011). Subsurface microbial populations interact with these remobilized carbon sources (Teske et al., 2014) under hydrothermal constraints that set Guaymas Basin apart from other systems supported by sedimentation of terrestrial or marine carbon sources.

The past ~50 y of scientific ocean drilling have shown that metabolite concentration and isotopic tracers are fundamental to constrain carbon cycle and subsurface biosphere processes operating throughout the sediment column (e.g., Heuer et al., 2009; Wehrmann et al., 2011; Hong et al., 2013). In the specific case of Guaymas Basin, the isotopic composition of the various carbon reservoirs provides information on the system response to varying organic carbon inputs, the meta-

bolic carbon transformations, and mass balance carbon inventories. As a contribution to the overall geochemical data, here we report the concentration and isotopic composition of dissolved inorganic carbon (DIC) in pore fluids from seven sites that encompass the thermal, lithologic, geochemical, and microbiological contrasting settings that were sampled and explored during the expedition (**Teske et al.**, 2021a; **Teske et al.**, 2021b).

2. Study sites

Site locations are illustrated in Figure **F1**. Below we present a short summary for site descriptions; a comprehensive report detailing characteristics of each site is given in **Teske et al.** (2021a).

2.1. Sites U1545 and U1546

The paired Sites U1545 and U1546 were drilled ~1 km from each other in the northern part of the basin to allow for a detailed assessment of the effect that thermal and hydrothermal alteration driven by sill intrusions can have on carbon cycling, mobilization, and metabolism. The sediment at both sites was described to be primarily a mixture of laminated diatom ooze and clay minerals with minor nannofossils, silt-sized siliciclastic particles, and authigenic minerals that include pyrite and clay- to silt-sized carbonate (micrite) particles (mainly dolomite). Discrete concretions and indurated limestone/dolomite intervals were reported at both sites below ~100 meters below seafloor (mbsf) (**Teske et al.**, 2021c; **Teske et al.**, 2021d).

Site U1545 recovered a deep-seated thin sill near the bottom of the hole, but the massive, deeply buried ~74 m thick sill at Site U1546 is expected to have a larger influence on the chemical and physical properties of the surrounding sediment. In particular, the combined biotic and abiotic sediment–water interactions resulting from the sill intrusion will affect carbon metabolic remobilization as well as sequestration in authigenic carbonate. These processes can be clarified with the data presented here.

2.2. Sites U1547 and U1548

Patterns of hydrothermal circulation at and around an active vent site called Ringvent (Teske et al., 2019) were investigated by drilling two sites in the central part of the northern Guaymas Basin. Site U1547 targeted the hot, shallow-emplaced sill at Ringvent. Site U1548 sampled the Ringvent

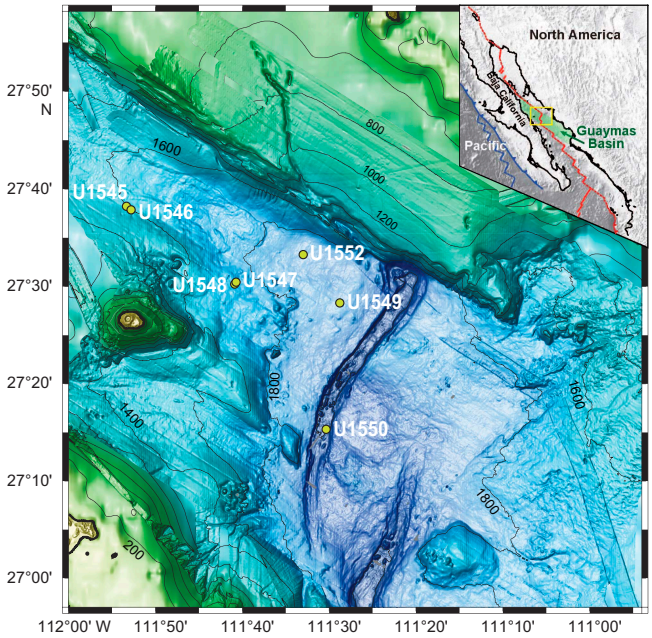

Figure F1. Study area and sample locations, Expedition 385. Modified from Teske et al. (2021a).

periphery with a series of holes drilled across the hydrothermal gradient outside the ring structure guided by the abrupt lateral change in seismic character observed in these sediments: Holes U1548A–U1548C are considered peripheral to the hot Ringvent sill, and Holes U1548D and U1548E recovered cooler sediments at a greater distance from Ringvent (**Teske et al.**, 2021e).

The sediments recovered at Sites U1547 and U1548 are dominated by diatom oozes, with a larger proportion of siliciclastic components relative to Sites U1545 and U1546. The sediment from the various holes drilled exhibits variations in the diagenetic stages of biogenic silica and authigenic carbonate precipitation, which may be responding to temperature-driven reactions associated with the Ringvent structure (**Teske et al.**, 2021e).

2.3. Sites U1549 and U1552

Site survey data at Sites U1549 and U1552 identified chemosynthetic cold-seep communities on the seafloor that point to the presence of methane seepage focused above the edges of underlying sills (Teske et al., 2021i). Both sites targeted similar surficial mound structures. Because of safety concerns related to the presence of free gas, Site U1549 was drilled peripheral to the seep center and is considered to be an off-axis reference site unaffected by advective flux (**Teske et al.**, 2021f). In contrast, Site U1552 aimed directly at an acoustically blanked chimney subseafloor structure indicative of active gas advection that fuels methane hydrate formation (**Teske et al.**, 2021h). The sedimentary section at these sites is composed of diatom oozes mixed with a significant proportion of sand- to silt-sized siliciclastic components, which in some cases occur in beds with vertical variability at meter scales.

2.4. Site U1550

Site U1550 was drilled in a fault-bounded spreading segment of the northern axial trough to sample sediments impacted by rapid fluid circulation driven by sill intrusion, as described in **Teske et al.** (2021g). The sedimentary section is classified into two lithologies determined by the relative proportions of biogenic (diatom clays with nannofossils) versus coarse-grained siliciclastic (sand and silt) components. The complex and disturbed section includes sediments, sedimentary rocks, and igneous rocks and displays a variety of features that have been used as evidence for the presence of mass-gravity flow deposits.

3. Analytical methods

Pore fluid extraction was conducted on the R/V *JOIDES Resolution* following the procedures described by **Teske et al.** (2021b). The squeezed pore fluids were collected in precleaned plastic syringes attached to the squeezing assembly and subsequently filtered through a 0.20 µm Gelman polysulfone disposable filter. Samples for isotopic composition of DIC were collected in 2 mL glass vials and were preserved with 10 µL of saturated $HgCl_2$.

The stable isotopic composition ($\delta^{13}C_{DIC}$) of the DIC was measured at the College of Earth, Ocean, and Atmospheric Sciences at Oregon State University (OSU-CEOAS; USA) using a technique specifically developed for analysis of small sample volumes and fully automated to maximize daily sample throughput for analysis of large data sets (Torres et al., 2005). The method uses a GasBench II headspace sampler online with a Finnigan DELTAplus-XL gas-source isotope ratio mass spectrometer housed at OSU-CEOAS. The precision of the $\delta^{13}C_{DIC}$ measurements based on replicate analyses of a $NaHCO_3$ stock solution is better than ±0.1‰. Instrument calibration was accomplished by comparison to National Institute of Standards and Technology (NIST)-8544 limestone (also known as NBS-19) prepared using a Kiel-III online acid digestion device, which yields isotopic values of 1.94‰ ± 0.02‰ for $\delta^{13}C$ (N = 25). These values compare well with the certified $\delta^{13}C_{DIC}$ value of 1.95‰. The gravimetrically prepared $NaHCO_3$ standards were used to create a concentration response factor for the output signal peak area in volt seconds (Vs) corresponding to the CO_2 evolved on the mass spectrometer, from which we derive the DIC concentration of each sample. Nominal concentration accuracy and precision were better than 2%.

4. Results

Results from the pore fluid analyses are presented in Table **T1** and illustrated in Figures **F2**, **F3**, **F4**, and **F5**, which in addition to our data include the downcore alkalinity profiles using data from **Teske et al.** (2021a).

4.1. Sites U1545 and U1546

At Site U1545, the DIC profile mirrors alkalinity, showing a maximum of 45.8 mM at 63.3 mbsf just below the depth of the sulfate–methane transition zone (SMTZ), as listed in **Teske et al.** (2021c). The carbon isotope values of the DIC also have a minimum at 44.3 mbsf with a value of −12.97‰ (Figure **F2**; Table **T1**). Below the SMTZ, DIC concentration decreases to a low value of 3.0 mM at 362.2 mbsf and $\delta^{13}C_{DIC}$ values gradually increase toward a maximum value of 15.38‰ in the deepest sample (Figure **F2**; Table **T1**). These profiles are in agreement with those typically observed in continental margins where anaerobic oxidation of methane releases bicarbonate enriched in ^{12}C at the SMTZ. Below this depth, methanogenesis leaves a DIC pool enriched in the heavier ^{13}C isotope; the decrease in DIC suggests consumption by carbonate precipitation, consistent with the observation of authigenic carbonates (micrite and dolomite) in the sediment (**Teske et al.**, 2021c). These results contrast with those at Site U1546, where the DIC and its isotopic composition show less variability at the SMTZ (110 mbsf). DIC reaches a maximum of 14.0 mM, and $\delta^{13}C_{DIC}$ reaches a minimum of −6.77‰, both at 82.8 mbsf (Figure **F2**; Table **T1**). These values suggest a lower rate of microbial consumption of methane relative to neighboring Site U1545, but persistent methanogenesis below the SMTZ is supported by $\delta^{13}C_{DIC}$ values that reach 12.34‰ at 328.9 mbsf. Uptake of DIC in carbonates is also apparent at this site where DIC concentrations reach a minimum of 1.4 mM at the bottom of the hole (Figure **F2**; Table **T1**).

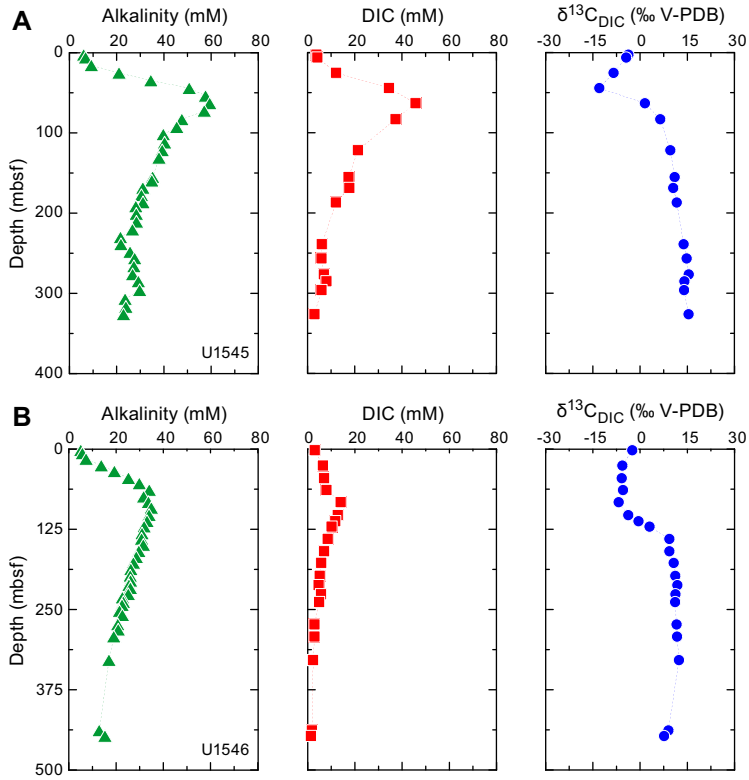

Figure F2. Downcore profiles of alkalinity, DIC, and $\delta^{13}C_{DIC}$, Sites (A) U1545 and (B) U1546. Alkalinity data from Teske et al. (2021c, 2021d). V-PDB = Vienna Peedee belemnite.

Table T1. DIC and its carbon isotopic composition, Expedition 385. **Download table in CSV format.**

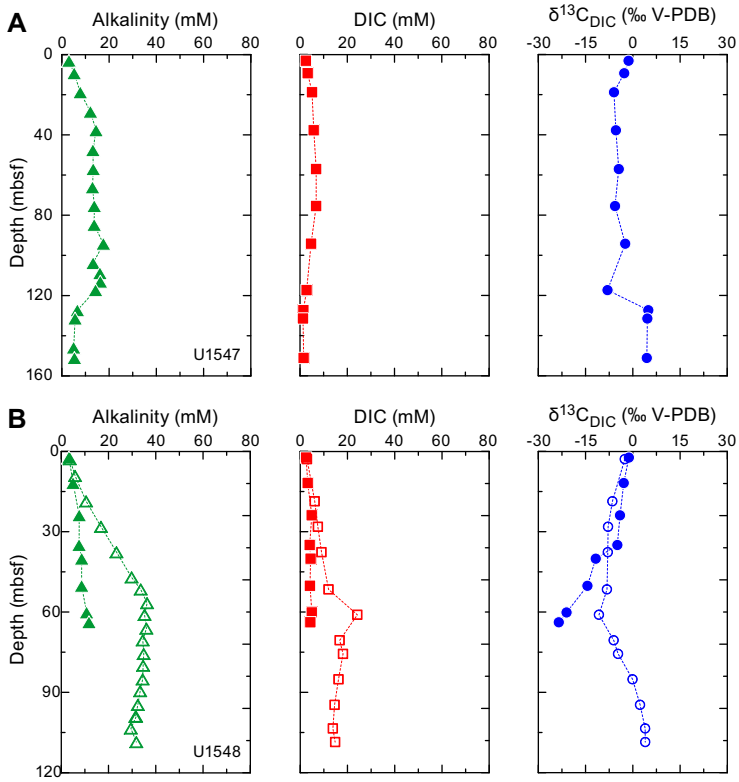

Figure F3. Downcore profiles of alkalinity, DIC, and $\delta^{13}C_{DIC}$, Sites (A) U1547 and (B) U1548. Solid symbols = Hole U1548C, open symbols = Hole U1548D. Alkalinity data from Teske et al. (2021e). V-PDB = Vienna Peedee belemnite.

4.2. Sites U1547 and U1548

Neither Site U1547 nor Site U1548, which were drilled at and around an active vent site, shows large changes in DIC concentration or its isotopic composition (Figure **F3**; Table **T1**). Consistent with the low alkalinity values reported at these sites (**Teske et al.**, 2021e), DIC at Site U1547 ranges 1.5 mM (15.1 mbsf) to 6.8 mM (57.0–75.5 mbsf). The carbon isotopic composition at this site ranges from −8.02‰ at 117.3 mbsf to positive values between 4.93‰ and 4.44‰ for the deepest samples between 127.3 and 151.1 mbsf. Although the $\delta^{13}C_{DIC}$ profile in Hole U1548C adjacent to Ringvent shows significant downcore depletion in ^{12}C ($\delta^{13}C_{DIC}$ of −23.50‰ at 63.8 mbsf), $\delta^{13}C_{DIC}$ in the companion Hole U1548D at a greater distance from Ringvent reaches only a local minimum of −10.74‰ (61.0 mbsf). In neither hole is there a significant enrichment in ^{13}C, with a maximum value of −1.25‰ at 2.3 mbsf in Hole U1548C and 3.94‰ at 108.6 mbsf in Hole U1548D. It is remarkable that $\delta^{13}C_{DIC}$ values become increasingly negative and reach −23.50‰ at the bottom of Hole U1548C; it is the most negative data point in the entire data set and more negative than in any SMTZ.

4.3. Sites U1549 and U1552

Sites U1549 and U1552 are characterized by very high concentrations of DIC, consistent with the high alkalinity values reported shipboard (**Teske et al.**, 2021f; **Teske et al.**, 2021h). DIC concentrations reach a maximum value of 76.0 mM at 83.0 mbsf at Site U1549 and 168.6 mM at 35.7 mbsf at Site U1552 (Figure **F4**; Table **T1**). The carbon isotopic composition at these sites shows the typical ^{13}C depletion at the SMTZ, reaching −17.66‰ at 25.6 mbsf at Site U1549 and −21.20‰ at 5.7 mbsf at Site U1552. Below the SMTZ, methanogenesis leads to a DIC pool enriched in ^{13}C, with a maximum value of 15.04‰ at 102.2 mbsf at Site U1549 and 22.64‰ at 35.7 mbsf at Site U1552 (Figure **F4**; Table **T1**).

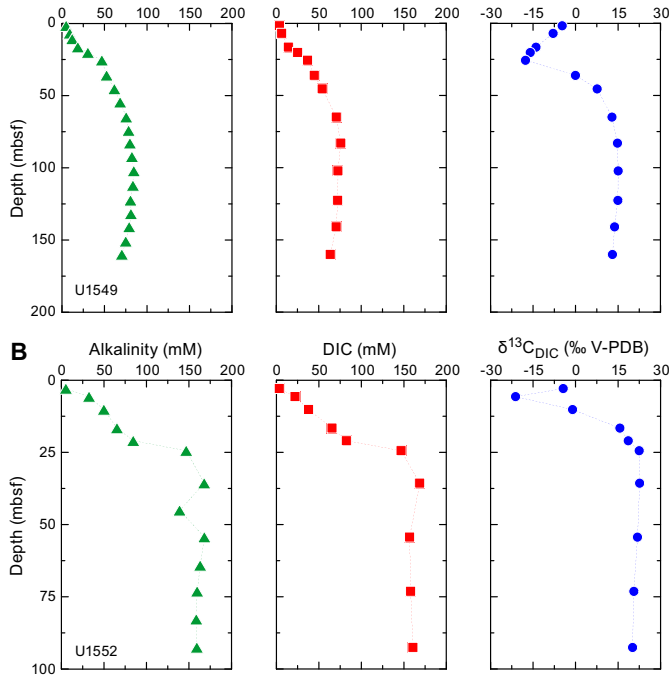

Figure F4. Downcore profiles of alkalinity, DIC, and $\delta^{13}C_{DIC}$, Sites (A) U1549 and (B) U1552. Alkalinity data from Teske et al. (2021f, 2021h). V-PDB = Vienna Peedee belemnite.

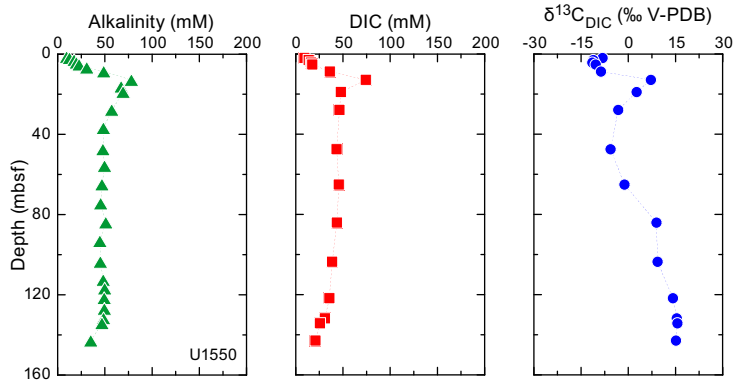

Figure F5. Downcore profiles of alkalinity, DIC, and $\delta^{13}C_{DIC}$, Site U1550. Alkalinity data from Teske et al. (2021g). V-PDB = Vienna Peedee belemnite.

4.4. Site U1550

At Site U1550, the DIC concentration increases from seawater values to a maximum value of 74.4 mM at 12.9 mbsf and then decreases to 21.0 mM at the bottom of the hole (Figure **F5**; Table **T1**). The isotopic composition of this pool shows more variability than typically observed, but in general the $\delta^{13}C_{DIC}$ shows its lowest value of –10.35‰ at 5.3 mbsf and a high value of 15.14‰ at 142.9 mbsf (Figure **F5**; Table **T1**).

5. Acknowledgments

This research used samples and data provided by the International Ocean Discovery Program (IODP), which is sponsored by the US National Science Foundation and participating countries. We acknowledge the outstanding efforts of the drilling personnel and the scientific parties of IODP Expedition 385. Without their hard work and dedication, none of these samples could have

been recovered for analysis. We thank Andy Ross for his assistance in generating these data. This research was funded by US Science Support Program postcruise research Award U1471A to Marta E. Torres and by the Korea Ministry of Oceans and Fisheries (NP2011-040) to Ji-Hoon Kim.

References

Einsele, G., Gieskes, J.M., Curray, J., Moore, D.M., Aguayo, E., Aubry, M.-P., Fornari, D., Guerrero, J., Kastner, M., Kelts, K., Lyle, M., Matoba, Y., Molina-Cruz, A., Niemitz, J., Rueda, J., Saunders, A., Schrader, H., Simoneit, B., and Vacquier, V., 1980. Intrusion of basaltic sills into highly porous sediments, and resulting hydrothermal activity. Nature, 283(5746):441–445. ‘Heuer, V.B., Pohlman, J.W., Torres, M.E., Elvert, M., and Hinrichs, K.-U., 2009. The stable carbon isotope biogeochemistry of acetate and other dissolved carbon species in deep sub-seafloor sediments at the northern Cascadia margin. Geochimica et Cosmochimica Acta, 73(11):3323–3336. **https://doi.org/10.1016/j.gca.2009.03.001**

Hong, W.-L., Torres, M.E., Kim, J.-H., Choi, J., and Bahk, J.-J., 2013. Carbon cycling within the sulfate-methane-transition-zone in marine sediments from the Ulleung Basin. Biogeochemistry, 115(1):129–148. **https://doi.org/10.1007/s10533-012-9824-y**

Lizarralde, D., Soule, S.A., Seewald, J.S., and Proskurowski, G., 2011. Carbon release by off-axis magmatism in a young sedimented spreading centre. Nature Geoscience, 4:50–54. **https://doi.org/10.1038/ngeo1006**

Teske, A., Callaghan, A.V., and LaRowe, D.E., 2014. Biosphere frontiers of subsurface life in the sedimented hydrothermal system of Guaymas Basin. Frontiers in Microbiology, 5:362. **https://doi.org/10.3389/fmicb.2014.00362**

Teske, A., Lizarralde, D., Höfig, T.W., Aiello, I.W., Ash, J.L., Bojanova, D.P., Buatier, M.D., Edgcomb, V.P., Galerne, C.Y., Gontharet, S., Heuer, V.B., Jiang, S., Kars, M.A.C., Khogenkumar Singh, S., Kim, J.-H., Koornneef, L.M.T., Marsaglia, K.M., Meyer, N.R., Morono, Y., Negrete-Aranda, R., Neumann, F., Pastor, L.C., Peña-Salinas, M.E., Pérez Cruz, L.L., Ran, L., Riboulleau, A., Sarao, J.A., Schubert, F., Stock, J.M., Toffin, L.M.A.A., Xie, W., Yamanaka, T., and Zhuang, G., 2021a. Expedition 385 summary. In Teske, A., Lizarralde, D., Höfig, T.W., and the Expedition 385 Scientists, Guaymas Basin Tectonics and Biosphere. Proceedings of the International Ocean Discovery Program, 385: College Station, TX (International Ocean Discovery Program). **https://doi.org/10.14379/iodp.proc.385.101.2021**

Teske, A., Lizarralde, D., Höfig, T.W., Aiello, I.W., Ash, J.L., Bojanova, D.P., Buatier, M.D., Edgcomb, V.P., Galerne, C.Y., Gontharet, S., Heuer, V.B., Jiang, S., Kars, M.A.C., Khogenkumar Singh, S., Kim, J.-H., Koornneef, L.M.T., Marsaglia, K.M., Meyer, N.R., Morono, Y., Negrete-Aranda, R., Neumann, F., Pastor, L.C., Peña-Salinas, M.E., Pérez Cruz, L.L., Ran, L., Riboulleau, A., Sarao, J.A., Schubert, F., Stock, J.M., Toffin, L.M.A.A., Xie, W., Yamanaka, T., and Zhuang, G., 2021b. Expedition 385 methods. In Teske, A., Lizarralde, D., Höfig, T.W., and the Expedition 385 Scientists, Guaymas Basin Tectonics and Biosphere. Proceedings of the International Ocean Discovery Program, 385: College Station, TX (International Ocean Discovery Program). **https://doi.org/10.14379/iodp.proc.385.102.2021**

Teske, A., Lizarralde, D., Höfig, T.W., Aiello, I.W., Ash, J.L., Bojanova, D.P., Buatier, M.D., Edgcomb, V.P., Galerne, C.Y., Gontharet, S., Heuer, V.B., Jiang, S., Kars, M.A.C., Khogenkumar Singh, S., Kim, J.-H., Koornneef, L.M.T., Marsaglia, K.M., Meyer, N.R., Morono, Y., Negrete-Aranda, R., Neumann, F., Pastor, L.C., Peña-Salinas, M.E., Pérez Cruz, L.L., Ran, L., Riboulleau, A., Sarao, J.A., Schubert, F., Stock, J.M., Toffin, L.M.A.A., Xie, W., Yamanaka, T., and Zhuang, G., 2021c. Site U1545. In Teske, A., Lizarralde, D., Höfig, T.W., and the Expedition 385 Scientists, Guaymas Basin Tectonics and Biosphere. Proceedings of the International Ocean Discovery Program, 385: College Station, TX (International Ocean Discovery Program). **https://doi.org/10.14379/iodp.proc.385.103.2021**

Teske, A., Lizarralde, D., Höfig, T.W., Aiello, I.W., Ash, J.L., Bojanova, D.P., Buatier, M.D., Edgcomb, V.P., Galerne, C.Y., Gontharet, S., Heuer, V.B., Jiang, S., Kars, M.A.C., Khogenkumar Singh, S., Kim, J.-H., Koornneef, L.M.T., Marsaglia, K.M., Meyer, N.R., Morono, Y., Negrete-Aranda, R., Neumann, F., Pastor, L.C., Peña-Salinas, M.E., Pérez Cruz, L.L., Ran, L., Riboulleau, A., Sarao, J.A., Schubert, F., Stock, J.M., Toffin, L.M.A.A., Xie, W., Yamanaka, T., and Zhuang, G., 2021d. Site U1546. In Teske, A., Lizarralde, D., Höfig, T.W., and the Expedition 385 Scientists, Guaymas Basin Tectonics and Biosphere. Proceedings of the International Ocean Discovery Program, 385: College Station, TX (International Ocean Discovery Program). **https://doi.org/10.14379/iodp.proc.385.104.2021**

Teske, A., Lizarralde, D., Höfig, T.W., Aiello, I.W., Ash, J.L., Bojanova, D.P., Buatier, M.D., Edgcomb, V.P., Galerne, C.Y., Gontharet, S., Heuer, V.B., Jiang, S., Kars, M.A.C., Khogenkumar Singh, S., Kim, J.-H., Koornneef, L.M.T., Marsaglia, K.M., Meyer, N.R., Morono, Y., Negrete-Aranda, R., Neumann, F., Pastor, L.C., Peña-Salinas, M.E., Pérez Cruz, L.L., Ran, L., Riboulleau, A., Sarao, J.A., Schubert, F., Stock, J.M., Toffin, L.M.A.A., Xie, W., Yamanaka, T., and Zhuang, G., 2021e. Sites U1547 and U1548. In Teske, A., Lizarralde, D., Höfig, T.W., and the Expedition 385 Scientists, Guaymas Basin Tectonics and Biosphere. Proceedings of the International Ocean Discovery Program, 385: College Station, TX (International Ocean Discovery Program). **https://doi.org/10.14379/iodp.proc.385.105.2021**

Teske, A., Lizarralde, D., Höfig, T.W., Aiello, I.W., Ash, J.L., Bojanova, D.P., Buatier, M.D., Edgcomb, V.P., Galerne, C.Y., Gontharet, S., Heuer, V.B., Jiang, S., Kars, M.A.C., Khogenkumar Singh, S., Kim, J.-H., Koornneef, L.M.T., Marsaglia, K.M., Meyer, N.R., Morono, Y., Negrete-Aranda, R., Neumann, F., Pastor, L.C., Peña-Salinas, M.E., Pérez Cruz, L.L., Ran, L., Riboulleau, A., Sarao, J.A., Schubert, F., Stock, J.M., Toffin, L.M.A.A., Xie, W., Yamanaka, T., and Zhuang, G., 2021f. Site U1549. In Teske, A., Lizarralde, D., Höfig, T.W., and the Expedition 385 Scientists, Guaymas Basin Tectonics and Biosphere. Proceedings of the International Ocean Discovery Program, 385: College Station, TX (International Ocean Discovery Program). **https://doi.org/10.14379/iodp.proc.385.106.2021**

Teske, A., Lizarralde, D., Höfig, T.W., Aiello, I.W., Ash, J.L., Bojanova, D.P., Buatier, M.D., Edgcomb, V.P., Galerne, C.Y., Gontharet, S., Heuer, V.B., Jiang, S., Kars, M.A.C., Khogenkumar Singh, S., Kim, J.-H., Koornneef, L.M.T., Marsaglia, K.M., Meyer, N.R., Morono, Y., Negrete-Aranda, R., Neumann, F., Pastor, L.C., Peña-Salinas, M.E., Pérez Cruz, L.L., Ran, L., Riboulleau, A., Sarao, J.A., Schubert, F., Stock, J.M., Toffin, L.M.A.A., Xie, W., Yamanaka, T., and Zhuang, G., 2021g. Site U1550. In Teske, A., Lizarralde, D., Höfig, T.W., and the Expedition 385 Scientists, Guaymas Basin Tectonics and Biosphere. Proceedings of the International Ocean Discovery Program, 385: College Station, TX (International Ocean Discovery Program). **https://doi.org/10.14379/iodp.proc.385.107.2021**

Teske, A., Lizarralde, D., Höfig, T.W., Aiello, I.W., Ash, J.L., Bojanova, D.P., Buatier, M.D., Edgcomb, V.P., Galerne, C.Y., Gontharet, S., Heuer, V.B., Jiang, S., Kars, M.A.C., Khogenkumar Singh, S., Kim, J.-H., Koornneef, L.M.T., Marsaglia, K.M., Meyer, N.R., Morono, Y., Negrete-Aranda, R., Neumann, F., Pastor, L.C., Peña-Salinas, M.E., Pérez Cruz, L.L., Ran, L., Riboulleau, A., Sarao, J.A., Schubert, F., Stock, J.M., Toffin, L.M.A.A., Xie, W., Yamanaka, T., and Zhuang, G., 2021h. Site U1552. In Teske, A., Lizarralde, D., Höfig, T.W., and the Expedition 385 Scientists, Guaymas Basin Tectonics and Biosphere. Proceedings of the International Ocean Discovery Program, 385: College Station, TX (International Ocean Discovery Program). **https://doi.org/10.14379/iodp.proc.385.109.2021**

Teske, A., McKay, L.J., Ravelo, A.C., Aiello, I., Mortera, C., Núñez-Useche, F., Canet, C., Chanton, J.P., Brunner, B., Hensen, C., Ramírez, G.A., Sibert, R.J., Turner, T., White, D., Chambers, C.R., Buckley, A., Joye, S.B., Soule, S.A., and Lizarralde, D., 2019. Characteristics and evolution of sill-driven off-axis hydrothermalism in Guaymas Basin – the Ringvent site. Scientific Reports, 9(1):13847. **https://doi.org/10.1038/s41598-019-50200-5**

Teske, A., Wegener, G., Chanton, J.P., White, D., MacGregor, B., Hoer, D., de Beer, D., Zhuang, G., Saxton, M.A., Joye, S.B., Lizarralde, D., Soule, S.A., and Ruff, S.E., 2021i. Microbial communities under distinct thermal and geochemical regimes in axial and off-axis sediments of Guaymas Basin. Frontiers in Microbiology, 12:633649. **https://doi.org/10.3389/fmicb.2021.633649**

Torres, M.E., Mix, A.C., and Rugh, W.D., 2005. Precise $\delta^{13}C$ analysis of dissolved inorganic carbon in natural waters using automated headspace sampling and continuous-flow mass spectrometry. Limnology and Oceanography: Methods, 3(8):349–360. **https://doi.org/10.4319/lom.2005.3.349**

Wehrmann, L.M., Risgaard-Petersen, N., Schrum, H.N., Walsh, E.A., Huh, Y., Ikehara, M., Pierre, C., D'Hondt, S., Ferdelman, T.G., Ravelo, A.C., Takahashi, K., and Alvarez Zarikian, C., 2011. Coupled organic and inorganic carbon cycling in the deep sub-sea floor sediment of the northeastern Bering Sea slope (IODP Exp. 323). Chemical Geology, 284(3):251–261. **https://doi.org/10.1016/j.chemgeo.2011.03.002**